2019

Spectroscopy of Neon for the Advanced Undergraduate Laboratory

H. C. Busch

M. B. Cooper
Old Dominion University

C. I. Sukenik
Old Dominion University, csukenik@odu.edu

Original Publication Citation

Busch, H. C., Cooper, M. B., & Sukenik, C. I. (2019). Spectroscopy of neon for the advanced undergraduate laboratory. *American Journal of Physics, 87*(3), 223-229. doi:10.1119/1.5088806

Spectroscopy of neon for the advanced undergraduate laboratory

H. C. Busch[a)]
Department of Chemistry, Physics and Astronomy, Georgia College and State University, Milledgeville, Georgia 31061

M. B. Cooper and C. I. Sukenik[b)]
Department of Physics, Old Dominion University, Norfolk, Virginia 23529

(Received 8 October 2018; accepted 29 December 2018)

We describe a spectroscopy experiment, suitable for upper-division laboratory courses, that investigates saturated absorption spectroscopy and polarization spectroscopy in a neon discharge. Both experiments use nearly identical components, allowing students to explore both techniques in a single apparatus. Furthermore, because the wavelength of the laser is in the visible part of the spectrum (640 nm), the experiment is well-suited for students with limited experience in optical alignment. The labs nicely complement a course in atomic or plasma physics, provide students with the opportunity to gain important technical skills in the area of optics and lasers, and can provide an introduction to radio-frequency electronics.
https://doi.org/10.1119/1.5088806

I. INTRODUCTION

The importance of the Advanced Laboratory course for undergraduate students has received increased attention over the last few years.[1–3] In addition to promoting a better understanding of a variety of topics within subfields of physics, the Advanced Laboratory also enables students to gain hands-on, technical skills. In the area of atomic, molecular and optical physics (AMO), experiments involving spectroscopy are a powerful educational component of any laboratory curriculum and can be used to elucidate material in upper-level special-topics courses.[4–10]

With the advent of inexpensive semiconductor diode lasers operating at 780 nm and the ability to fabricate homebuilt, tunable lasers,[11,12] Doppler-free saturated absorption spectroscopy[13] (SAS) of rubidium (Rb) has now become a staple offering of many undergraduate lab courses.[14–17] This experiment is rich in atomic physics, requires only a modest amount of equipment, can largely be assembled with off-the-shelf optical components, and works well even with a simple, homebuilt semiconductor diode laser. In addition, rubidium is a good candidate for this Advanced Laboratory experiment because its vapor pressure at room temperature is sufficient to perform experiments without the need for heating the vapor cell or producing an atomic beam. One drawback of performing Rb SAS, though, is that 780 nm is at the edge of the wavelength range that is visible to the naked eye and so viewing faint beams of this wavelength requires a dark room, the aid of an infrared (IR) viewing card, or possibly even an IR viewer. These conditions are not ideal for beginning students.

One option to enable students to investigate SAS while developing laser and optical alignment skills using visible light is to swap lithium (Li) for Rb and use a 671 nm diode laser. To get the required vapor pressure, however, requires considerable heating of a specialized vapor cell.[19] Another option is to investigate the 640 nm transition in neon (Ne).

As we describe in this paper, we have developed a spectroscopy experiment for the Advanced Laboratory that investigates SAS and another spectroscopic technique, known as polarization spectroscopy[13,20] (PS), in Ne. Both experiments can be performed with a nearly identical set of components. There are three stable isotopes of neon: ^{20}Ne (90.48%), ^{21}Ne (0.27%), and ^{22}Ne (9.25%), with natural abundances given in parentheses; our experiment performs spectroscopy on ^{20}Ne. The optical transition studied is the $3s[3/2]_2 \rightarrow 3p[5/2]_3$ transition at 640.2 nm (wavelength in air) as shown in Fig. 1. This red wavelength is easily visible even at very low laser powers.

The Rb and Ne SAS experiments have many common features, but an important difference (in addition to the required laser wavelength) is that the involved Rb transition goes from the atom's ground state ($5s_{1/2}$) to its first excited state ($5p_{3/2}$), whereas the utilized Ne transition takes place between two excited states. Laser excitation of Ne from its ground state to its first excited state, via an allowed electric dipole transition, is not practical because the required (ultraviolet) wavelength is 74 nm. This constraint is common to all noble gases. However, once neon is excited, the transition from the $3s[3/2]_2$ with $J = 2$ to the ground state with $J = 0$ does not satisfy the following selection rules for allowed electric dipole transitions: $\Delta J = 0, \pm 1$, but $J = 0 \not\rightarrow 0$. As a result, the $3s[3/2]_2$ state decays by the much weaker magnetic quadrupole decay and has a lifetime of $\sim$15 s.[21] This long-lived "metastable" state is denoted as Ne* and it plays the same role as the $5s_{1/2}$ ground state in Rb SAS.

Because laser excitation is impractical, excitation from the ground state to higher-energy metastable states in noble gases is usually done using a direct-current (dc) or radio-frequency (rf) discharge. In the experiments described below, we used a rf discharge operated at $\sim$80 MHz to promote Ne atoms to the $3s[3/2]_2$ state. The discharge requirement does add some additional equipment to the apparatus as compared to Rb SAS. However, the inclusion of a *plasma* in our experiment provides students with an opportunity to learn about plasma physics (including a connection to the physics of the helium-neon laser) and rf electronics.[22]

II. THEORY

A. Saturated absorption spectroscopy

Saturated absorption spectroscopy[13] is a pump-probe technique for gas samples, which allows one to remove Doppler broadening of absorption peaks, thereby greatly improving

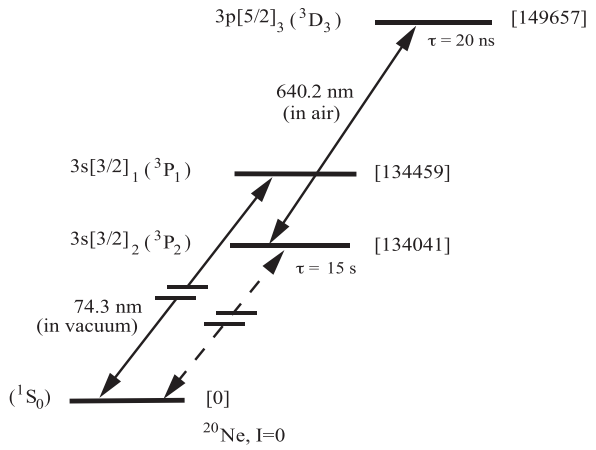

Fig. 1. Partial energy level diagram for neon (not to scale). Atomic levels are labelled in both LS coupling and Racah notation (Ref. 18). Even isotopes of noble gases have nuclear spin $I=0$ and therefore do not possess hyperfine structure. Energy is shown in brackets in units of wavenumbers [cm^{-1}] ($1\,\mathrm{eV}=8065.5\,\mathrm{cm}^{-1}$). The $3s[3/2]_2$ metastable state decays via a magnetic quadrupole (M2) transition (dashed arrow) and has a lifetime of ~15 s.

the resolution of spectra. Doppler broadening of the absorption peaks results from the thermal motion of atoms or molecules in the gas. Here, we highlight the essential physics of the technique. A weak laser beam is sent through a gas of atoms, usually at room temperature or in a heated cell, and the absorption of that beam is monitored, typically with a photodiode. This beam will be called the "probe beam." Assume that, when an atom is at rest, it will absorb the probe beam at the resonant frequency ν_0. Then, as a result of the Maxwell-Boltzmann distribution of atomic velocities in a gas sample, the sample's absorption spectrum will be broadened because, for each atom with its own particular velocity component v_z along the direction of laser propagation, the laser will need to be tuned to $\nu=\nu_0(1+v_z/c)$ in the laboratory frame in order to be resonant in the atom's reference frame, where c is the speed of light. Therefore, a laser on resonance in the lab frame appears out of resonance to most atoms, whose v_z velocity distribution is proportional to $e^{-Mv_z^2/2k_BT}$, where M is the mass of the atom, k_B is Boltzmann's constant, and T is the temperature. As the laser is scanned, this distribution will give rise, in the low absorption limit, to a Gaussian absorption profile whose full-width at half maximum is given by

$$\Delta\nu_{1/2}=\nu_0\sqrt{8k_BT\ln 2/Mc^2}. \tag{1}$$

This is known as the *Doppler width*. For neon at room temperature $T=300\,\mathrm{K}$, the Doppler width is ~1.3 GHz. The hotter the gas, the greater the thermal distribution of velocities and the broader the observed spectrum.

Now consider a second, stronger laser beam (called the "pump beam") of identical frequency to the probe beam, also sent through the cell, but counter-propagating to the probe laser beam. If the strong pump beam excites an atom that otherwise would be excited by the weak probe beam, that atom is no longer available for excitation by the probe beam and absorption of the probe beam will decrease. For most laser frequencies within the Doppler-broadened absorption profile this will not be the case because for a particular moving atom, one of the laser beams will be "red-shifted" (down in frequency) and the other "blue-shifted" (up in frequency) owing to the fact that the beams are counter-propagating. However, for a certain velocity class of atoms, namely, those with $v_z=0$, there is no Doppler shift to either beam and excitation by the strong beam will modify the probe absorption. In other words, the SAS technique monitors the change to the absorption of a weak probe beam due to a strong pump beam that is interacting with the specific velocity class of atoms for which there is no Doppler shift.

As the laser scans, a broad Doppler absorption peak is observed peppered with narrow features. These features appear at the resonance frequencies of the atomic transitions and have widths that can be comparable to the natural linewidth of the transition. In practice, these features are often broader than the natural linewidth due to power-broadening by the laser beams.[23] If γ is the natural linewidth, then the power broadened linewidth γ_{rad} will be

$$\gamma_{rad}=\gamma\sqrt{1+I/I_{sat}}, \tag{2}$$

where I is the intensity of the laser and I_{sat} is the saturation intensity, defined as $I_{sat}=\pi hc/(3\lambda^3\tau)$, where λ is the wavelength of the transition and τ is the excited state lifetime. I_{sat} is defined such that when $I=I_{sat}$, there is a 25% chance that the atom is in the excited state. The saturation intensity for the $3s[3/2]_2\rightarrow 3p[5/2]_3$ transition in neon, studied here, is $I_{sat}=4.22\,\mathrm{mW/cm}^2$ and $\gamma=8.47\,\mathrm{MHz}$.[24] Note that, with the multilevel structure of atoms, optical pumping can be important, yielding a spectrum that differs from the one predicted by a simple two-level atom model.[15,25] Furthermore, for some atoms, it is possible to observe narrow features in the spectra that do not correspond to resonant frequencies of the atom but rather appear at frequencies that are midway between two resonant frequencies. These are known as *crossover peaks* and arise when both the pump and probe beams interact with the same atom, but excite different transitions.[13] Because ^{20}Ne does not have hyperfine structure, crossover peaks are not observed in the experiments described here (in contrast to SAS in rubidium), but optical pumping that redistributes the population of magnetic sublevels is present.

B. Polarization spectroscopy

Polarization spectroscopy is also a sub-Doppler spectroscopic technique usually accomplished with two counter-propagating laser beams of different intensity, and with both beams derived from the same laser. In PS, the polarization of the strong pump beam is set to be circular. The circularly polarized pump beam modifies the optical properties of the atomic gas. This effect can then be interrogated by the weak probe beam. The signature of PS is a dispersion-like signal that results when the different polarization components of the probe beam are subtracted after traversing the gas. Typically, a weak linearly polarized probe beam is superimposed on a circularly polarized counter-propagating pump beam in a gas or vapor cell.[26–29]

The observed signal is derived from the change in the polarization of the probe laser beam after it traverses the gas. This change is due to the optical anisotropy induced by the stronger pump beam, which arises from optical pumping that redistributes the population of the magnetic sublevels. The incident linearly polarized probe beam can be decomposed into two beams of opposite circular polarization (usually denoted σ^+ and σ^-). As a result of both optical pumping and

saturation effects, the pump beam places atoms into a non-uniform population distribution of the magnetic sublevels, which in turn gives rise to a difference in index of refraction (optical birefringence) and absorption (circular dichroism) between the two polarization components of the probe beam. The circular dichroism causes the probe beam to have an elliptical polarization upon exiting the gas, whereas the optical birefringence gives rise to a rotation in the axis of polarization. If the probe beam is sent to a linear polarization analyzer after exiting the cell, and the two polarization channels are subtracted, the resulting signal is dispersion-like and can be used for laser stabilization without the need for any modulation. This technique has been applied in alkali-metal vapors, in gas discharges, and in hollow cathode lamps.[30–37] As we describe below, we use a hollow cathode lamp (HCL), but do not operate it as such. Instead, we create a radio-frequency discharge using the neon buffer gas that is in the lamp.

For the probe beam traveling in the z-direction, the PS signal I_{signal} derived from its horizontal (x) and vertical (y) linear components will be

$$I_{signal} = I_y - I_x, \\ = I_0 e^{-\alpha L} \cos\left(2\phi + \frac{\omega}{c} L\Delta n\right). \quad (3)$$

Here, $\Delta n = n_+ - n_-$ with $n_\pm$ being the refractive indices of the neon for circular polarization components of the laser that drive $\sigma^\pm$ transitions and $\alpha = \frac{1}{2}(\alpha_+ + \alpha_-)$ with $\alpha_\pm$ being the absorption coefficients, respectively. L is the length of the gas cell. Finally, ω is the angular frequency of the laser light, I_0 is the intensity of the light before the cell, and ϕ is the polarization of the probe beam with respect to the x-axis.[30] We have neglected any birefringence from the cell windows (see Ref. 30 to include these effects). In most cases, it is a good assumption that both $\Delta\alpha$ and Δn are "small" such that $L\Delta\alpha \ll 1$ and $(\omega/c)L\Delta n \ll 1$. With the laser scanned across an isolated resonance, $\Delta\alpha$ can be written as a Lorentzian function of the form

$$\Delta\alpha(\omega) = \frac{\Delta\alpha_0}{1 + x^2}, \quad (4)$$

where $\Delta\alpha_0$ is the maximum difference in absorption at resonance line center and $x = (\omega_0 - \omega)/(\Gamma/2)$, with Γ being the linewidth of the resonance. For $\phi = \pi/4$ and using the Kramers-Kronig dispersion relation[13] to relate Δn to $\Delta\alpha$, we can write an approximation for the observed signal as

$$I_{signal} = -I_0 e^{-\alpha L}\left(L\Delta\alpha_0 \frac{x}{1 + x^2}\right). \quad (5)$$

III. EQUIPMENT

A. Optical layout

The equipment and optical layout for both the SAS and PS experiments are nearly identical, enabling students to perform both experiments as part of a single Advanced Laboratory module. We used a mix of commercial and homebuilt controllers for the laser, largely making use of existing equipment in our Advanced Laboratory. We give manufacturer and model numbers for reference only. We begin with the arrangement for the SAS experiment as shown in Fig. 2. A visible 639 nm laser diode (Opnext HL6358MG) was placed in a homebuilt external cavity diode laser (ECDL) operating in Littrow configuration with a linewidth of ~1 MHz.[12] The diffraction grating had 1800 lines/mm (Thorlabs GR13-1850). Coarse tuning of the laser was achieved by rotating the diffraction grating. Finer tuning was achieved with a combination of current and temperature adjustments to the laser diode as well as a voltage supplied to a piezoelectric transducer (PZT) installed on the diffraction grating mount that enabled precise mechanical adjustment of the cavity. The PZT (Thorlabs AE0203D04) was driven by an amplifier/driver (Burleigh PZ-150M) that in turn was controlled by a homebuilt scan controller. We used a commercial diode laser current controller (ILX Lightwave LDX-3412) and a homebuilt temperature controller. The laser was tuned to 640.2 nm (air wavelength), corresponding to the $3s[3/2]_2 \rightarrow 3p[5/2]_3$ transition. The PZT allowed the laser to be scanned in frequency with a mode-hop free range of ~500 MHz. After leaving the ECDL, the laser beam passed through an optical isolator (Electro-Optics Technology) to prevent feedback and a plate beamsplitter to pick off a small amount of light directed to a Fabry-Perot spectrum analyzer. The spectrum analyzer (Spectra Physics, Model 470-03, with a free spectral range of 2 GHz), was used to monitor the ECDL to ensure single longitudinal mode operation and to calibrate the frequency scan. We had a commercial spectrum analyzer on hand, but one can also build an inexpensive instrument for the lab.[38] A mirror on a flip mount was used, when needed, to intercept the laser beam and direct it to a fiber optic cable that was sent to a wavelength meter to assist with initial tuning of the ECDL. If a precision wavelength meter is not available, a

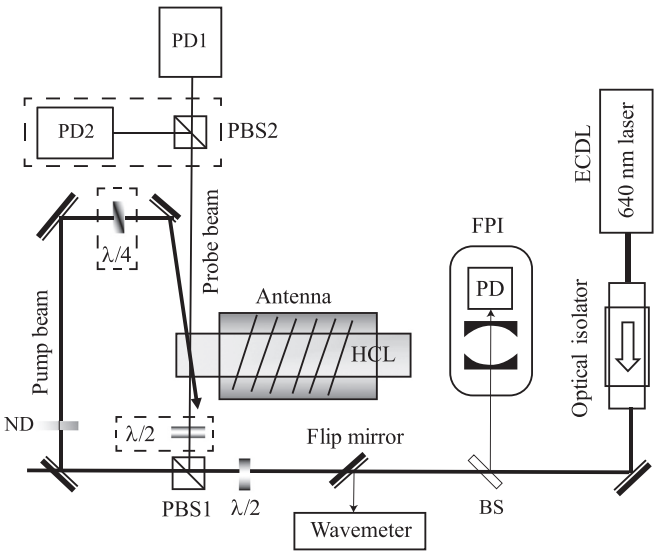

Fig. 2. Schematic of the optical layout for both the saturated absorption spectroscopy experiment and the polarization spectroscopy experiment. Components in the dashed boxes are employed for polarization spectroscopy only. Both experiments share most components and can be performed with minimal modification to the optical layout. Key: ECDL: External cavity diode laser; PD: Photodiode; PBS: Polarizing beamsplitter cube; BS: Beamsplitter; ND: Neutral density filter; FPI: Fabry-Perot Interferometer (optical spectrum analyzer); HCL: Hollow cathode lamp; $\lambda/2$: half waveplate; $\lambda/4$: quarter waveplate. The HCL is shown mounted horizontally for clarity, but was actually mounted vertically in the experiment to save space and keep reflections from curved surfaces in the horizontal plane.

monochromator or even a simple homebuilt grating spectrometer can be used for coarse tuning.[39] The laser passes through a half-waveplate before impinging on a broadband polarizing beamsplitter cube (PBS1). The waveplate allows the laser power to be split between the weak probe beam and the strong pump beam. A separate neutral density filter wheel placed in the path of the strong pump beam allows for independent adjustment of the pump beam power. After traversing the discharge cell (in this case, a HCL), the weak beam is directed onto a photodiode (PD1). Our photodiode assembly uses an OPT101P (Texas Instruments) which is a combined monolithic photodiode and transimpedance amplifier on a single chip. The HCL we used was manufactured by Thermo Electron Corp (P/N 9423 393 31241). This unit was a 6 in. long cylinder with a flat window at one end and electrical feedthroughs at the other end; it had a 1.25 in. long section with a diameter of 1 in. at the window end and the remainder of the lamp was 1.5 in. in diameter. The laser beams enter and exit the HCL through the 1 in. diameter curved surface near the window and, as a result, the spatial quality of the laser beam is degraded and the divergence increased after traversing the cell. Because the probe beams need only travel a few inches before reaching the detector, however, this effect was not a significant issue. In Fig. 2, the HCL is shown mounted horizontally for clarity. In the experiment, the HCL was actually mounted vertically. Vertical mounting reduces the footprint of the setup and also keeps all reflections from the curved lamp surface in the original horizontal plane, which is important for safety.

Only minor modifications to the optical setup are required for the polarization spectroscopy experiment. The additional required components are shown inside the dashed boxes in Fig. 2. A polarizing beamsplitter cube (PBS2, Newport 05FC16PB.5), which acts as a polarization analyzer, is placed in the path of the probe beam, between the discharge cell and PD1 and a second photodiode (PD2) is added. Output from each photodiode is sent to a separate channel of an oscilloscope and is subtracted to provide the PS signal. This difference signal can be viewed directly on the oscilloscope by using the built-in math functions common to most digital oscilloscopes or the signals from each PD can be individually saved and the data processed in software afterwards. If the signal is to be further used for another application (such as laser frequency stabilization), then the two channels will need to be subtracted with a simple electronic circuit. In addition, two waveplates are added. A half-wave plate is installed after PBS1, but before the discharge, and is used to rotate the vertical polarization of the probe beam by $\sim 45^\circ$ in order to balance the light sent to the two photodiodes in the absence of the pump beam. A quarter-wave plate is added just before the "D" folding mirror of the pump beam to circularly polarize the pump light. Ideally the circularly polarized pump beam would not be reflected off of a mirror before being sent to the discharge because birefringence of the mirror can distort the light polarization. Geometrical constraints made it difficult to avoid the placement of this mirror between the waveplate and the discharge cell. Though not ideal, the arrangement works fine; the counter-propagating probe and pump beams cross with a small angle of less than 2°.

B. Neon plasma

As mentioned above, metastable Ne atoms are created in a rf discharge. While commercial gas cells are readily available for both alkali metal atoms and noble gases, we found it convenient and cost effective to use a commercial hollow-cathode lamp to create the discharge. Most commercial HCLs (manufactured for installation in spectrometers) are filled with neon, irrespective of the cathode element. Lamps filled with argon or krypton are also available, though harder to find. One benefit of using a commercial HCL as the gas cell source is that "spent" discharge tubes that have been removed from spectrometers are usually just discarded and can be repurposed for use here. Further details about options for the discharge cell can be found in the Appendix.

A block diagram of the rf electronics is shown in Fig. 3. The antenna used to transmit the rf waves to the discharge was a 15-turn helical coil (3 in. long, $\sim$1.75 in. in diameter) of 14-gauge copper magnet wire placed inside a cylindrical 3 in. diameter copper tube.[40] The antenna is similar to the design analyzed in Ref. 41. The coil pitch and number of turns can be easily modified to accommodate different discharge frequency ranges.[42] The discharge does not need to be run at the resonant frequency of the antenna circuit in order to produce Ne*. We have used this type of antenna (with various coil pitches and total turns) for discharges ranging from tens of MHz to 1 GHz. Tuning of the rf frequency once the discharge has been established reveals specific frequencies where a given antenna/HCL combination prefers to operate, but we have found that the discharge will typically work over several hundred MHz, thereby lessening the tolerances on coil geometry during construction. A voltage controlled oscillator (VCO, Mini-Circuits ZOS-100+) with an output of 10 dBm, and operating at $\sim$80 MHz, was sent to a voltage-controlled attenuator (Mini-Circuits ZX73-2500-S+), which allowed adjustment of the power ultimately delivered to the discharge. The signal was then amplified with a rf power amplifier (Mini-Circuits TVA-R5-13) and passed through a rf power meter (Bird Technologies, Model 43) before being sent to the antenna that surrounded the HCL tube. We did not use an "antenna tuner" (impedance matcher) in this arrangement, though one could be added just past the power amplifier to cut down on reflected power. Typical forward power was measured to be a few Watts. The discharge sometimes started on its own when the rf power was applied. Other times, we ignited the discharge using a piezo sparker extracted from a common butane barbecue lighter. With the

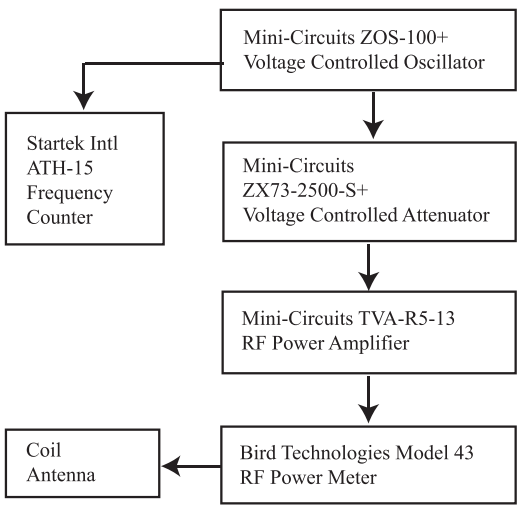

Fig. 3. Block diagram of the radio-frequency electronics used to create the neon discharge.

HCL inserted into the rf antenna, the discharge running and the laser on resonance, the rf power was adjusted to obtain a plasma plume in the lamp with a strong visible "pencil" of fluorescence where the laser passed through the discharge.

IV. EXPERIMENTAL RESULTS

In Fig. 4, we show the observed saturation absorption peak for the 640 nm transition in ^{20}Ne. The laser beam had an elliptical spatial profile with $1/e^2$ diameters of 3.8 mm × 1.8 mm. Here, the probe beam power was ∼60 μW while the pump beam power was ∼1.6 mW. The FWHM of a Lorentzian function fitted to the peak is ∼64 MHz, which is larger than would be explained by power broadening alone, suggesting that other mechanisms such as collisional broadening may also be contributing to the observed linewidth. The pressure in our HCL was not known, which is one disadvantage of using a lamp of this type; precise specifications from the manufacturer are often limited.

With modifications to the SAS setup described earlier, we were able to perform polarization spectroscopy of ^{20}Ne. The half-waveplate just before PBS1 was adjusted so that the probe laser power was set to ∼30 μW. The pump laser power was 3.6 mW. We were able to observe a signal with powers as low as 1.6 mW for the pump and 9 μW for the probe. A neutral density filter was used to vary the intensity of the pump beam to observe the effect of pump power on the PS signal strength. The PS signal was largest when the pump beam was at the maximum power available. Figure 5 shows the PS signal. Here, the output of each photodiode is shown, along with the difference signal that displays the characteristic PS dispersive shape. Note that if the quarter-waveplate were rotated by 90°, thereby changing the pump laser polarization helicity, the PS signal would be inverted. This feature is convenient when using the signal to frequency stabilize (i.e., lock) a laser and when the locking electronics require a specific slope of the error signal.

V. CONCLUSION

We have described a spectroscopy experiment for the Advanced Laboratory that explores saturated absorption spectroscopy and polarization spectroscopy of metastable neon produced in an rf discharge, using a nearly identical apparatus for both. Both experiments use 640 nm light. The visible wavelength used in these experiments is better suited for training students with limited experience in optical alignment in comparison to similar experiments that use a near-infrared wavelength (which is challenging to see). The labs nicely complement a course in atomic or plasma physics, provide students with the opportunity to gain important technical skills in the area of optics and lasers, and offer an introduction to the radio-frequency electronics used to produce the discharge. With the addition of a power meter or calibrated photodiode, students can also explore the intensity dependence of the observed signal linewidth. In addition, either experiment can be expanded to be a component in a separate laboratory investigating frequency stabilization (locking) of lasers or the discussion of polarization spectroscopy can be utilized to modify an existing Rb saturated absorption spectroscopy apparatus to investigate polarization spectroscopy in alkali metal atoms. Finally, we plan to extend the mode-hop-free frequency tuning range of our laser[44] in order to enable students to measure the isotope shift between ^{20}Ne and ^{22}Ne as part of the same laboratory module.[45]

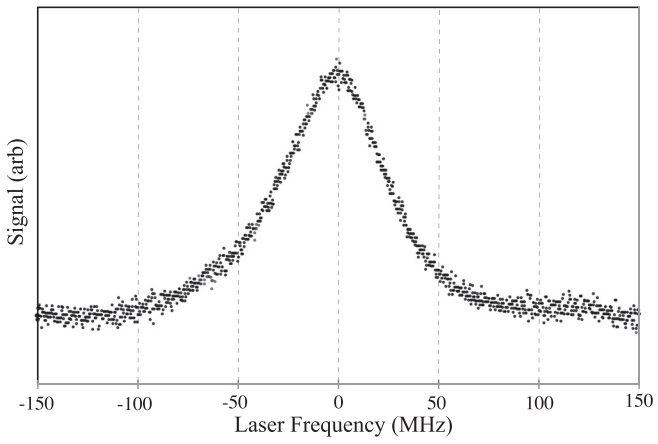

Fig. 4. Signal obtained for the neon Saturated Absorption Spectroscopy experiment. Unlike rubidium, which has many peaks because of hyperfine structure, ^{20}Ne has no hyperfine structure and the saturation absorption spectrum has only a single peak.

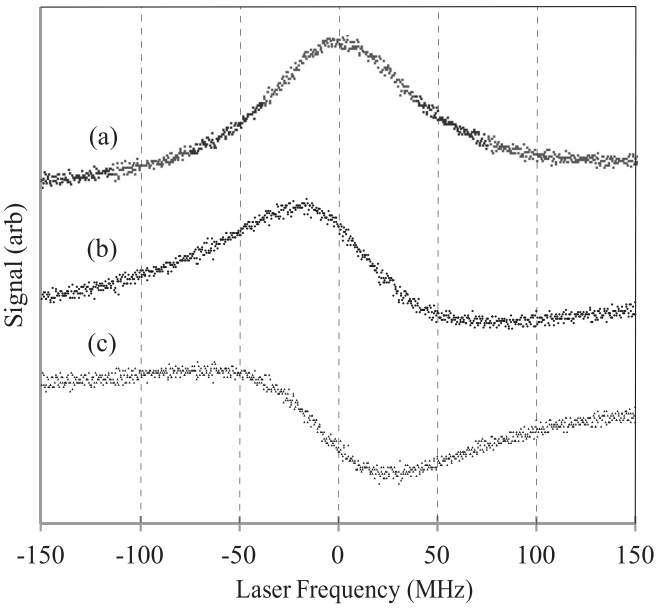

Fig. 5. Signal obtained for the neon Polarization Spectroscopy experiment. (a) Signal from PD1; (b) signal from PD2; (c) difference when trace (a) is subtracted from trace (b).

ACKNOWLEDGMENTS

Support provided by the Virginia Space Grant Consortium, Old Dominion University and Georgia College & State University.

APPENDIX: CHOOSING A DISCHARGE CELL

For this experiment, we chose to create an rf discharge in a commercial hollow cathode lamp. We have found that commercial noble gas cells (with fills of ∼200 mTorr) tend to go bad over time in a discharge, especially at frequencies below a few hundred MHz. Homebuilt cells that include

some form of getter mechanism tend to last longer as do cells operated in the GHz frequency range. It should be noted that when developing this advanced lab, we investigated running the HCL with a dc current (as is done in spectrometers), using a HCL supply (Emco, Model HC2012). While we were able to obtain spectra, we found a number of drawbacks to this arrangement. First, many tube geometries did not afford good optical access to the discharge region. Second, in order to obtain a suitable population of Ne* for the experiment, we had to run the current beyond the rated limit, which resulted in sputtering of the cathode that coated the walls of the tube, thereby attenuating the laser beams over time. On the other hand, using a rf discharge to create Ne* in the HCL significantly increased the ease of optical alignment, while eliminating the sputtering issue.

[a]Electronic mail: hauke.busch@gcsu.edu
[b]Electronic mail: csukenik@odu.edu

[1]AAPT Recommendations for the Undergraduate Physics Laboratory Curriculum (American Association of Physics Teachers, 2014).
[2]Benjamin M. Zwickl, Noah Finkelstein, and H. J. Lewandowski, "Incorporating learning goals about modeling into an upper-division physics laboratory experiment," Am. J. Phys. **82**(9), 876–882 (2014).
[3]Benjamin M. Zwickl, Noah Finkelstein, and H. J. Lewandowski, "The process of transforming an advanced lab course: Goals, curriculum, and assessments," Am. J. Phys. **81**(1), 63–70 (2013).
[4]L. Ivanjek, P. S. Shaffer, L. C. McDermott, M. Planinic, and D. Veza, "Research as a guide for curriculum development: An example from introductory spectroscopy. I. Identifying student difficulties with atomic emission spectra," Am J. Phys. **83**(1), 85–90 (2015).
[5]Jennifer Blue, Burcin S. Bayram, and S. Douglas Marcum, "Creating, implementing, and sustaining an advanced optical spectroscopy laboratory course," Am. J. Phys. **78**(5), 503–509 (2010).
[6]R. S. Conroy, A. Carleton, A. Carruthers, B. D. Sinclair, C. F. Rae, and K. Dholakia, "A visible extended cavity diode laser for the undergraduate laboratory," Am. J. Phys. **68**(10), 925–931 (2000).
[7]Abraham J. Olson, Evan J. Carlson, and Shannon K. Mayer "Two-photon spectroscopy of rubidium using a grating feedback diode laser," Am. J. Phys. **74**(3), 218–222 (2006).
[8]U. Gustafsson, J. Alnis, and S. Svanberg, "Atomic Spectroscopy with violet laser diodes," Am. J. Phys. **68**(7), 660–664 (2000).
[9]Dmitry Budker, Donald J. Orlando, and Valeriy Yashchuk, "Nonlinear laser spectroscopy and magneto-optics" Am. J. Phys. **67**(7), 584–592 (1999).
[10]Dietrich Krebs, Stefan Pabst, and Robin Santra, "Introducing many-body physics using atomic spectroscopy," Am. J. Phys. **82**(2), 113–122 (2014).
[11]Carl E. Wieman and Leo Hollberg, "Using diode lasers for atomic physics," Rev. Sci. Instrum. **62**(1), 1–20 (1991).
[12]C. J. Hawthorn, K. P. Weber, and R. E. Scholten, "Littrow configuration tunable external cavity diode laser with fixed direction output beam," Rev. Sci. Instrum. **72**(12), 4477–4479 (2001).
[13]W. Demtröder, *Laser Spectroscopy*, 4th ed. (Springer-Verlag, Berlin Heidelberg, 2008), Chap. 2.
[14]K. B. MacAdam, A. Steinbach, and C. Wieman, "A narrow band tunable diode-laser system with grating feedback and a saturated absorption spectrometer for Cs and Rb," Am. J. Phys. **60**(12), 1098–1111 (1992).
[15]David A. Smith and Ifan G. Hughes, "The role of hyperfine pumping in multilevel systems exhibiting saturated absorption," Am. J. Phys. **72**(5), 631–637 (2004).
[16]Daryl W. Preston, "Doppler-free saturated absorption: Laser spectroscopy," Am. J. Phys. **64**(11), 1432–1436 (1996).
[17]K. Razdan and D. A. Van Baak, "Demonstrating optical saturation and velocity selection in rubidium vapor," Am. J. Phys. **67**(9), 832–836 (1999).
[18]L. Radziemski, "Spectroscopic notation for the energy levels of helium and neon," Opt. News **15**(1), 15–16 (1989).
[19]K. G. Libbrecht, R. A. Boyd, P. A. Willems, T. L. Gustavson, and D. K. Kim, "Teaching physics with 670 nm diode lasers-construction of stabilized lasers and lithium cells," Am. J. Phys. **63**(8), 729–737 (1995).
[20]C. Wieman and T. W. Hänsch, "Doppler-free laser polarization spectroscopy," Phys. Rev. Lett. **36**(20), 1170–1173 (1976).
[21]Martin Zinner, Peter Spoden, Tobias Kraemer, Gerhard Birkl, and Wolfgang Ertmer, "Precision measurement of the metastable $^3P_2$ lifetime of neon," Phys. Rev. A **67**(1), 010501R (2003).
[22]Stephanie A. Wissel, Andrew Zwicker, Jerry Ross, and Sophia Gershman, "The use of dc glow discharges as undergraduate educational tools," Am. J. Phys. **81**(9), 663–669 (2013).
[23]A. J. Hachtel, J. D. Kleykamp, D. G. Kane, M. D. Marshall, B. W. Worth, J. T. Barkeloo, J. C. B. Kangara, J. C. Camenisch, M. C. Gillette, and S. Bali, "An undergraduate measurement of radiative broadening in atomic vapor," Am. J. Phys. **80**(8), 740–743 (2012); , "Erratum: An undergraduate measurement of radiative broadening in atomic vapor [Am. J. Phys. **80**, 740 (2012)]," **81**(6), 471 (2013).
[24]Harold J. Metcalf and Peter van der Straten, *Laser Cooling and Trapping* (Springer, New York, 1999).
[25]Ben E. Sherlock and Ifan G. Hughes, "How weak is a weak probe in laser spectroscopy?," Am. J. Phys. **77**(2), 111–115 (2009).
[26]H. D. Do, G. Moon, and H.-R. Noh, "Polarization spectroscopy of rubidium atoms: Theory and experiment," Phys. Rev. A **77**(3), 032513(6) (2008).
[27]P. Kulatunga, H. C. Busch, L. R. Andrews, and C. I. Sukenik, "Two-color polarization spectroscopy of rubidium," Opt. Commun. **285**(12), 2851–2853 (2012).
[28]M. L. Harris, C. S. Adams, S. L. Cornish, I. C. McLeod, E. Tarleton, and I. G. Hughes, "Polarization spectroscopy in rubidium and cesium," Phys. Rev. A **73**(6), 062509(8) (2006).
[29]D. Groswasser, A. Waxman, M. Givon, G. Aviv, Y. Japha, M. Keil, and R. Folman, "Retroreflecting polarization spectroscopy enabling miniaturization," Rev. Sci. Instrum. **80**(9), 093103(3) (2009).
[30]C. P. Pearman, C. S. Adams, S. G. Cox, P. F. Griffin, D. A. Smith, and I. G. Hughes, "Polarization spectroscopy of a closed atomic transition: applications to laser frequency locking," J. Phys. B: At. Mol. Opt. Phys. **35**, 5141–5151 (2002).
[31]Y. Yoshikawa, T. Umeki, T. Mukae, Y. Torii, and T. Kuga, "Frequency stabilization of a laser diode with use of light-induced birefringence in an atomic vapor," Appl. Opt. **42**(33), 6645–6649 (2003).
[32]V. B. Tiwari, S. Singh, S. R. Mishra, H. S. Rawat, and S. C. Mehendale, "Laser frequency stabilization using Doppler-free bi-polarization spectroscopy," Opt. Commun. **263**(2), 249–255 (2006).
[33]Y. B. Kale, V. B. Tiwari, S. Singh, S. R. Mishra, and H. S. Rawat, "Velocity selective bipolarization spectroscopy for laser cooling of metastable krypton atoms," J. Opt. Soc. Am. **31**(11), 2531–2539 (2014).
[34]Teng Wu, Xiang Peng, Wei Gong, Yuanzhi Zhan, Zaisheng Lin, Bin Luo, and Hong Guo, "Observation and optimization of ^{4}He atomic polarization spectroscopy," Opt. Lett. **38**(6), 986–988 (2013).
[35]Jackson Ang'ong'a and Bryce Gadway, "Polarization spectroscopy of atomic erbium in a hollow cathode lamp," J. Phys. B: At. Mol. Opt. Phys. **51**(4) 045003(10) (2018).
[36]S. Zhu, T. Chen, X. Li, and Y. Wang, "Polarization spectroscopy of $^1S_0$-$^1P_1$ transition of neutral ytterbium isotopes in hollow cathode lamp," J. Opt. Soc. Am. B **31**(10), 2302–2309 (2014).
[37]B. Smeets, R. Bosch, P. van der Straten, E. Tesligte, R. Scholten, H. Beijerinck, and K. van Leeuwen, "Laser frequency stabilization using an Fe-Ar hollow cathode discharge cell," Appl. Phys. B **76**(8), 815–819 (2003).
[38]Thomas Moses, Mark, Wolak, Fafim Chandurwala, and Tenzing Shaw, "A simpler scanning Fabry-Perot interferometer for high-resolution spectroscopy experiments," Am. J. Phys. **83**(7), 656–659 (2015).
[39]James D. White and Robert E. Scholten, "Compact diffraction grating laser wavemeter with sub-picometer accuracy and picowatt sensitivity using a webcam imaging sensor," Rev. Sci. Instrum. **83**(11), 113104(4) (2012).
[40]C. Y. Chen, K. Bailey, Y. M. Li, T. P. O'Connor, and Z.-T. Lu, "Beam of metastable krypton atoms extracted from a rf-driven discharge," Rev. Sci. Instrum. **72**(1), 271–272 (2001).
[41]W. W. Macapine and R. O. Schildknecht, "Coaxial resonators with helical inner conductor," Proc. IRE **47**(12), 2099–2105 (1959).
[42]We note that an alternate, cost-effective setup is to run the discharge at ~150 MHz, corresponding to the 2 m amateur radio band and use components specifically designed for the amateur radio community. One

can also use a microwave discharge (Ref. 43), using components derived from a commercial microwave oven and a homebuilt microwave cavity.
[43]Y. Ding, K. Bailey, A. M. Davis, S.-M. Hu, Z.-T. Lu, and T. P. OConnor "Beam of metastable krypton atoms extracted from a microwave-driven discharge," Rev. Sci. Instrum. **77**(12), 126105(2) (2006).
[44]S. Charles Doret, "Simple, low-noise piezo driver with feed-forward for broad tuning of external cavity diode lasers," Rev. Sci. Instrum. **89**(2), 023102(5) (2018).
[45]B. Ohayon, G. Gumpel, and G. Ron, "Measurement of the ^{20,22}Ne $^3P_2$–$^3D_3$ transition isotope shift using a single, phase-modulated laser beam," J. Phys. B: At. Mol. Opt. Phys. **50**(5), 055401(5) (2017).

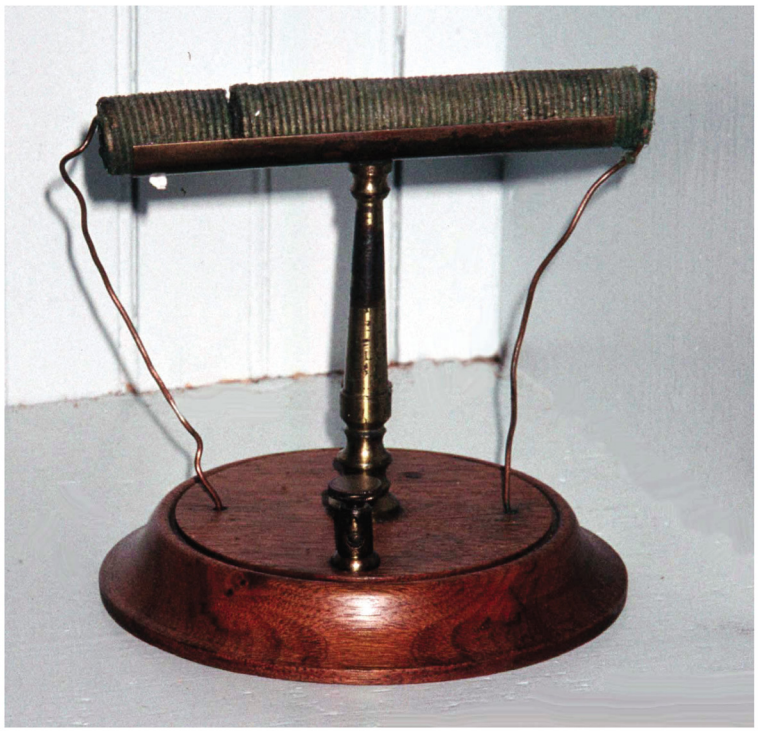

Horizontal Electromagnet

This apparatus list listed at $2 to $3 in the 1842 edition of Daniel Davis's *Manual of Magnetism*. Davis spends a fair amount of text explaining how the terminals of the battery must be connected to the helix to provide North and South Magnetic Poles. The one in my own collection I use with various rods inserted into the core of the helix. Paper clips attracted to the ends of the rod give a measure of the magnetic field that is produced. My favorite is a brass rod that is plated with nickel-silver or chrome, which looks as if it ought to be magnetized, but is not. The instrument in the picture is in the collection of Transylvania University in Lexington, Kentucky. (Picture and Text by Thomas B. Greenslade, Jr., Kenyon College.)